The Journal of Experimental Biology 210, 1742-1751
Published by The Company of Biologists 2007
doi:10.1242/jeb.001701

Aerodynamics of wing-assisted incline running in birds

Bret W. Tobalske[1,*] and Kenneth P. Dial[2]

[1]*Department of Biology, University of Portland, 5000 North Willamette Boulevard, Portland, OR 97203, USA and* [2]*Flight Laboratory, Division of Biological Sciences, University of Montana, 32 Campus Drive, Missoula, MT 59812, USA*

*Author for correspondence (e-mail: tobalske@up.edu)

Accepted 12 February 2007

Summary

Wing-assisted incline running (WAIR) is a form of locomotion in which a bird flaps its wings to aid its hindlimbs in climbing a slope. WAIR is used for escape in ground birds, and the ontogeny of this behavior in precocial birds has been suggested to represent a model analogous to transitional adaptive states during the evolution of powered avian flight. To begin to reveal the aerodynamics of flap-running, we used digital particle image velocimetry (DPIV) and measured air velocity, vorticity, circulation and added mass in the wake of chukar partridge *Alectoris chukar* as they engaged in WAIR (incline 65–85°; *N*=7 birds) and ascending flight (85°, *N*=2). To estimate lift and impulse, we coupled our DPIV data with three-dimensional wing kinematics from a companion study. The ontogeny of lift production was evaluated using three age classes: baby birds incapable of flight [6–8 days post hatching (d.p.h.)] and volant juveniles (25–28 days) and adults (45+ days). All three age classes of birds, including baby birds with partially emerged, symmetrical wing feathers, generated circulation with their wings and exhibited a wake structure that consisted of discrete vortex rings shed once per downstroke. Impulse of the vortex rings during WAIR was directed 45±5° relative to horizontal and 21±4° relative to the substrate. Absolute values of circulation in vortex cores and induced velocity increased with increasing age. Normalized circulation was similar among all ages in WAIR but 67% greater in adults during flight compared with flap-running. Estimated lift during WAIR was 6.6% of body weight in babies and between 63 and 86% of body weight in juveniles and adults. During flight, average lift was 110% of body weight. Our results reveal for the first time that lift from the wings, rather than wing inertia or profile drag, is primarily responsible for accelerating the body toward the substrate during WAIR, and that partially developed wings, not yet capable of flight, can produce useful lift during WAIR. We predict that neuromuscular control or power output, rather than external wing morphology, constrain the onset of flight ability during development in birds.

Key words: vorticity, circulation, added mass, lift, digital particle image velocimetry, ontogeny.

Introduction

Wing-assisted incline running (WAIR) is a form of escape behavior in birds that consists of flapping the wings during climbing (Dial, 2003; Dial et al., 2006). It is commonly used by ground-dwelling species such as the Galliformes when they have access to a sloped terrain (cliff, boulder, tree, etc.), and may also be common among nestlings of a diverse array of bird species (K.P.D., unpublished observation). During flapping flight the wings produce lift, normal to the incurrent velocity on the wing, which functions to support body weight and to produce thrust that opposes profile and parasite drag on the wings and body (Rayner, 1988; Norberg, 1990). As gravity dominates the force balance even during fast flight in vertebrates, net lift during steady flapping flight is oriented primarily upward (Rayner, 1988). In contrast, during WAIR it is hypothesized that lift from the wings functions primarily as thrust that accelerates the body toward the surface of the substrate being climbed, thereby increasing friction and aiding the feet in gaining purchase. Previous studies using kinematics, accelerometers and force plates have provided data in support of this hypothesis, but uncertainty remains about the aerodynamics of flap-running. Stroke-plane angles are oriented toward the substrate during the early phase of downstroke (Dial, 2003; Dial et al., 2006; Segre, 2006), and the body is accelerated toward the substrate during most of the wingbeat cycle (Bundle and Dial, 2003), but it has not been established whether such acceleration is due to lift, profile drag or inertia of the wings. One objective of the present study was to reveal the aerodynamic function of the wings for adults, juveniles, and even baby birds (6–8 days)

during WAIR using digital particle image velocimetry (DPIV).

Although WAIR is an intriguing escape behavior in adult birds, it emerges as a particularly fascinating behavior when the implications of flap-running are considered relative to the ontogeny and, potentially, the evolution of flight. Like many ground-dwelling birds, chukar partridge (*Alectoris chukar*; Gray 1830; hereafter 'chukar') exhibit precocial development. Baby chukar, covered in down, can walk away from their nest upon hatching. Their flight feathers emerge over several weeks, and they can fly approximately at 20 days post hatching (d.p.h.) when the flight feathers are fully emerged (Dial et al., 2006; Segre, 2006). Within 6–8 d.p.h., baby chukars have partially emerged, symmetrical wing feathers. These babies will use WAIR even though they are unable to fly, and they will continue to use WAIR throughout the rest of their development (Segre, 2006). The majority of bird species are altricial in their development, so the young leave the nest and fly for the first time using flight feathers that are nearly identical to those in the adult. Thus, WAIR in precocial species offers a unique opportunity to study the ontogeny of lift development in birds. Our second objective with the present investigation was to test whether the aerodynamics of the developing wing are the same across age classes of chukar.

If partially developed wings in precocial birds are reasonably analogous to the incipient wings that the presumed ancestors of modern birds possessed, then the ontogeny of WAIR in extant species offers a novel, testable biomechanical model for the origin of powered flight in birds (Bundle and Dial, 2003; Dial, 2003; Dial et al., 2006). This model assumes that development in external wing morphology is representative of the transitional adaptive stages (Bock, 1965) that led to the complex structure of the extant avian wing. An obvious limitation of the model is uncertainty in how extant avian neuromuscular control and kinematics compare with ancestral forms. Nonetheless, our present effort to document the aerodynamics of WAIR in baby chukar might provide new insight into how an ancestral incipient wing that was not capable of supporting flight may have been an exaptation (Gould and Vrba, 1982) originally used solely for WAIR.

Materials and methods

Birds and experimental design

Chukars *Alectoris chukar* Gray 1830 (*N*=7, Table 1, Fig. 1) used in this study were wild-type, captive-bred birds of three age classes: baby (6–8 d.p.h.), juvenile (25–28 days) and adult (45+ days). All housing and experimental procedures were approved by the Institutional Animal Care and Use Committee (IACUC) of the University of Portland and the University of Montana. We obtained morphometrics (Table 1) using standard techniques (e.g. Tobalske et al., 2005). The chukars were hatched and reared at the Flight Laboratory at Fort Missoula, University of Montana with continuous access to food and water *ad libitum*. Baby birds were housed in heated nest boxes, and juveniles and adults were housed in an outdoor aviary

Table 1. *Morphometric data for Alectoris chukar*

Variable	Age class		
	Baby	Juvenile	Adult
Body mass (g)	24.1±0.8	222±76	605±42
Single wing length (cm)	5.8±0.1	19±2	24.0±0.8
Wing span (cm)	15±1	44±5	56±2
Average wing chord (cm)	2.4±0.1	7±1	9±1
Aspect ratio	6.0±0.2	6.5±0.8	6.4±0.8
Single wing area (cm^2)	14±1	130±26	212±19
Aerodynamic area of both wings and body (cm^2)	36±5	297±63	499±69
Wing loading ($N\ m^{-2}$)	67±12	72±11	121±21
Disc loading ($N\ m^{-2}$)	14±3	14±3	24±2

Values are means ± s.d., *N*=2 babies, 5 juveniles and 2 adults.

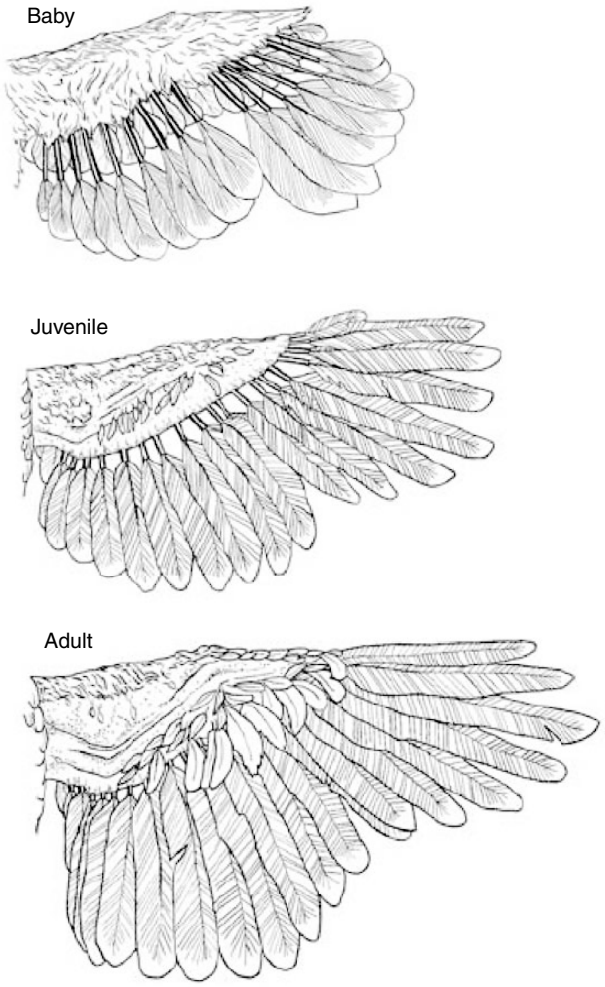

Fig. 1. Wing morphology in three age classes of chukar *Alectoris chukar*: babies (6–8 d.p.h.), juveniles (25–28 days), and adults (45+ days), which were used to study WAIR and flight. The wings are scaled so that the musculoskeletal portions are the same length. Adapted from Dial et al. (Dial et al., 2006).

6.2 m×15.2 m×3.9 m (width×length×height). Half of the experiments took place at the University of Portland (average

air density, ρ=1.15 kg m^{-3}), and half took place at the University of Montana (ρ=1.12 kg m^{-3}). The birds were transported between institutions using a private jet.

We used previously established methods for eliciting WAIR and flight (Bundle and Dial, 2003; Dial, 2003; Dial et al., 2006; Segre, 2006). Inclines, made of wooden boards, were 15 cm×45 cm×2 cm (width×length×thickness) for babies and 25 cm×2 m×2 cm (width×length×thickness) for juveniles and adults. With a refuge box at the top of an incline and 60-grit sand paper providing for traction, the birds climbed at the maximum slope for which we could obtain repeated runs. Average incline angle relative to horizontal was 65±0° in babies, 74±7° in juveniles, and 80±0° in adults (Fig. 2). To elicit flight in adults with a climb angle of approximately 80°, we removed the incline and released the bird by hand below the refuge box. We sampled the flights in the middle of the climb during the interval in which the birds were climbing approximately at a steady rate. We recorded and analyzed 138 WAIR trials and 11 flights.

Digital particle image velocimetry

For recording and analysis of DPIV data, we used a LaVison GmBH (Goettingen, Germany) DPIV system running DaVis 7.1 software. We used a dual-cavity pulsed 50-mJ Nd:YAG laser illuminate a flow field 3 mm thick, with planar dimensions spanning a field that was 17×23 cm for babies and 41×54 cm in juveniles and adults. The illumination field was caudal to the bird, parasagittal and mid-wing at the middle of downstroke (Spedding et al., 2003a; Warrick et al., 2005). We verified the location of the bird and the motion of its wings relative to the illumination field using a synchronized high-speed video camera (Redlake PCI-2000, San Diego, CA, USA) sampling at 250 Hz and located dorsal to the animal's line of travel. We seeded the air with particles of olive oil (<1 μm in diameter) generated at a rate of 7×10^{10} particles s^{-1} using a vaporizer fitted with a Laskin nozzle. Particle illumination was recorded using a 1376×1040 pixel, charged-coupled-device (CCD) camera placed perpendicular to the illumination field, and DPIV samples were obtained at 5 Hz.

To calculate particle velocity, we used cross-correlation of paired images with an elapsed time between images (Δt) of 500 μs for babies and 325 μs for juveniles and adults. Average particle separation was 6 pixels in the center of the animal's wake. We employed an adaptive multipass with an initial interrogation area of 64×64 pixels and final area of 16×16 pixels with 50% overlap. Vector fields were post-processed using a median filter (strong removal if difference relative to average >2*r.m.s. of neighbours and iterative reinsertion if <3*r.m.s. of neighbours), removal of groups with <5 vectors, fill of all empty spaces by interpolation, and one pass of 3×3 smoothing. We estimate minimum error in velocity measurements was 5.0±0.5%, including contributions due to a correlation peak of 0.1 pixels, optical distortion and particle-fluid infidelity (Raffel et al., 2000; Spedding et al., 2003b).

Subsequent analysis focused upon vortex cores and the

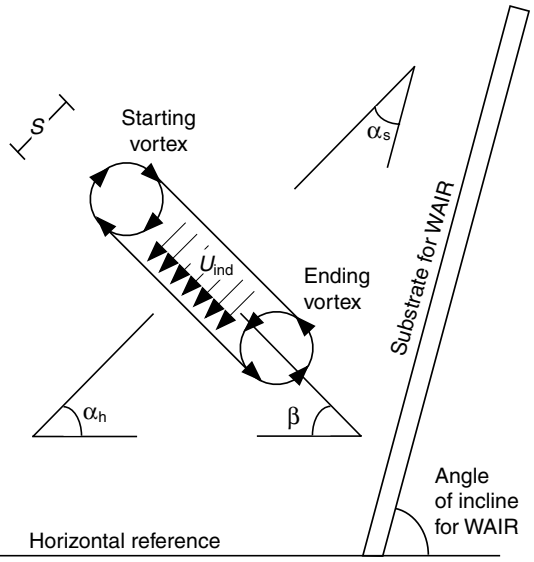

Fig. 2. Representation of the cross-section of a vortex in the wake of a bird engaged in WAIR including some of the variables measured in the wake vortices. U_{ind}, induced velocity in the momentum jet; α_h, impulse angle of wake vortex relative to horizontal; α_s, impulse angle of wake vortex relative to substrate; β, inclination angle of vortex; *S*, width of vortex.

velocity of the jet between the cores observed in the wake 1–5 chord lengths away from the base of the animal's wings (Fig. 2 and Fig. 3A). We used streamlines (Fig. 3B), drawn with vectors expressed relative to average velocity, to inform our selection of regions of vorticity. Vorticity (ω, in s^{-1}) was computed using post-processed vector fields as rot*z* (*dy*/*dx*). We treated as background noise and masked from subsequent analysis $|\omega|$<3s.d. of $|\omega|$ in the free-stream (Fig. 3C,D). To measure circulation (Γ, m^2 s^{-1}) in vortex cores, we initially used one of two methods adapted from Spedding et al. (Spedding et al., 2003a). First, we integrated ω with respect to area for all above-threshold, contiguous, same-sign ω about a given peak (ω_{max}), giving Γ_c (Fig. 3C,D). Second, we integrated all same-sign ω in a given DPIV field within 1.5 chord lengths (*c*) of peak ω to measure Γ_a. This method involved some subjectivity, and again was informed by the appearance of streamlines (Fig. 3B).

We considered each negatively signed vortex core deposited in the wake during early downstroke to represent the cross-section of a starting vortex (Figs 2, 3) shed from the trailing edge of the wing, equal in magnitude but opposite in sign from the bound vortex on the wing as lift development began during downstroke (Batchelor, 1967; Norberg, 1990; Spedding et al., 2003a). Similarly, we considered each positively signed vortex core deposited in the wake during late downstroke to represent the cross-section of an ending vortex shed from the trailing edge of the wing. Observed vortex cores may have represented portions of trailing tip vortices rather than starting or stopping vortices (Spedding et al., 2003a; Warrick et al., 2005), but the distinction was not relevant for our analyses as we assumed the

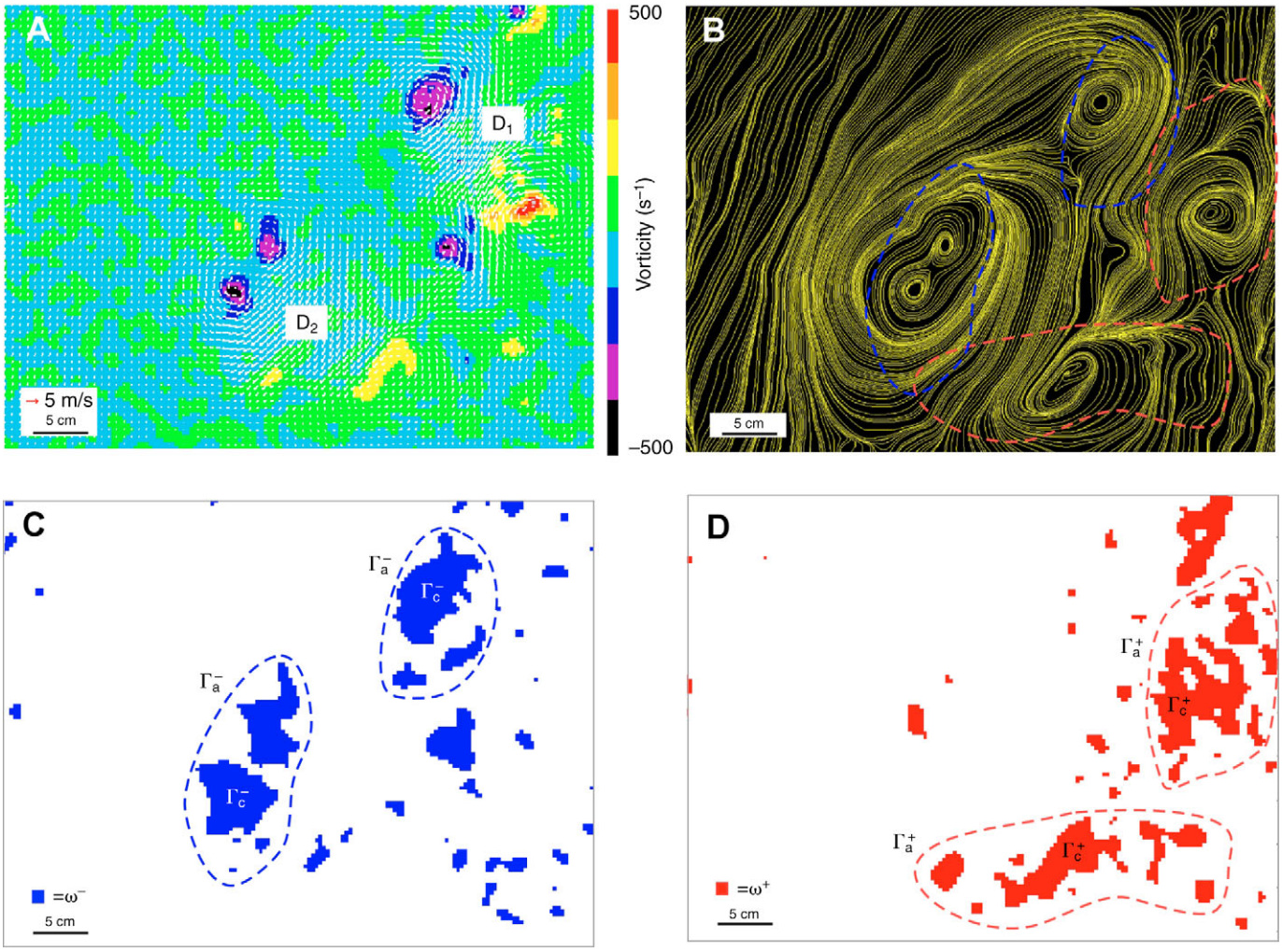

Fig. 3. Method used for identifying vortex cores and measuring circulation (Γ) in the wake of chukar *Alectoris chukar* as revealed using DPIV in a parasagittal plane at the mid-wing. In this instance, a juvenile chukar, no longer visible in the image, used WAIR to move upwards and toward the right through the illumination plane at an angle of 80°. Movements of its wings left vorticity (ω) in the wake that was concentrated into two presumptive vortex loops, one per downstroke (D_1 and D_2), which were transected by the illumination plane. (A) Velocity vectors, expressed relative to average velocity, and with backround ω. (B) Streamlines associated with the vector field. Broken lines indicate regions sampled for ω (blue=starting vortex, red=ending vortex). (C) Above-threshold ω^- (blue) and (D) above threshold ω^+ (red) was integrated with respect to area to measure contiguous circulation (Γ_c^- and Γ_c^+) or all circulation presumed to be associated with the core (Γ_a^- and Γ_a^+).

wake vortices rolled up into the form of planar elliptical loops (see estimation of lift, below).

As in Spedding et al. (Spedding et al., 2003a), Γ_c produced an estimate of average lift that was insufficient to support weight (i.e. match gravitational acceleration of the body at 9.805 m s^{-2}) during flight at a steady rate of climb (71±3% for Γ_c^- and 103±26% for Γ_c^+). During WAIR and flight, $|\Gamma_c^+|$ was significantly greater $|\Gamma_c^-|$ within what we interpreted to be a single vortex loop (paired *t*-test, P=0.0193; d.f.=8). We viewed this pattern as being inconsistent with the Kelvin–Helmholtz Circulation Theorem, which posits that circulation is constant within a given vortex, regardless of whether the vortex is a closed-loop or ends on a substrate (Batchelor, 1967). These problems were not apparent with $|\Gamma_a^-|$ and $|\Gamma_a^+|$, thus, we abandoned further use of Γ_c and hereafter report only Γ_a.

Far-field induced velocity (U_{ind}, Fig. 2 and Fig. 3A) in the jet between vortex cores was sampled midway between ω_{max}^- and ω_{max}^+ using an interrogation area 2 cm×2 cm for babies and 4 cm×4 cm for juveniles and adults. U_{ind} was probably greater, by some unmeasured amount, than the induced velocity at the wing (Ellington, 1984; Sane, 2006). We were unable to measure U_{ind} at the wing because the wings and body, and reflection of laser light, obscured near-field flow patterns. Direction of vortex impulse was considered to be normal to a line including ω_{max}^- and ω_{max}^+. We report acute angles of vortex impulse relative to horizontal (α_h, in degrees, Fig. 2) and relative to slope of incline (α_s, in degrees) along with the inclination angle of wake vortex relative to horizontal (β).

We estimated average lift by coupling our DPIV data with three-dimensional (3D) kinematic data obtained from the same

Table 2. *Kinematic data for Alectoris chukar engaged in wing-assisted incline running (WAIR) and flight*

	Age class			
Variable	Baby	Juvenile	Adult	Adult (flight)
Body velocity (U_b; m s^{-1})	0.6	1.2	1.5	1.4
Wingbeat duration (T; s)	0.110	0.069	0.073	0.073
Downstroke duration (t; s)	0.052	0.028	0.033	0.033
Elliptical loop area (S; m^2)	0.0076	0.0922	0.1324	0.1567

Values are means, N=1 per age class except N=2 for adults (flight).

age classes of chukars and reported in detail elsewhere (Segre, 2006) (Table 2). Added mass of the vortex wake was estimated using Dabiri's method (Dabiri, 2005). We made a number of simplifying assumptions in this effort, so caution is warranted when interpreting these estimates. Following Spedding et al. (Spedding et al., 2003a) and Warrick et al. (Warrick et al., 2005), we assumed that a single vortex loop shed per downstroke was planar and that no contraction occurred during wake development. Thus, the major and minor axes of an elliptical vortex loop were defined using the 3D excursion of the wing tips during downstroke. Average lift during the entire wingbeat (L) was estimated as:

$$L = \rho(A\Gamma_a + \bar{c}ASU_v) / T , \quad (1)$$

where A is the area of the vortex loop, $\bar{c}$ is added-mass coefficient, S is vortex width (Fig. 2), U_v is self-induced vortex velocity and T is wingbeat duration (Dabiri, 2005). To facilitate comparisons with previous accelerometer data (Bundle and Dial, 2003), we also computed L_d, the mean lift during downstroke by substituting T_d, downstroke duration (s) for T in Eqn 1.

The most appropriate method for measuring the added mass of the vortex wake (the second term in Eqn 1) involves the use of a Lagrangian frame of reference in which the trajectories of fluid particles are tracked over time (Dabiri, 2005; Dabiri et al., 2006; Shadden et al., 2006). This requires a time series of DPIV images. Our DPIV images were obtained at 5 Hz, the limit for our system, so we were unable to undertake a Lagrangian analysis. Instead, we assumed $\bar{c}$=0.72, which is the added-mass coefficient reported for an elliptical vortex (Dabiri, 2005). We measured S as the average diameter of observed vortex cores, and we measured U_v as observed rate of translation of ω_{max} in the subset (N=39) of our DPIV samples in which the same vortex core appeared in consecutive images.

Wake vortex ratio (W_a), a dimensionless index of the relative contribution of vortex added mass to the overall estimate of L was calculated according to Dabiri (Dabiri, 2005):

$$W_a = \bar{c}SU_v / \Gamma_a . \quad (2)$$

To remove the effects of body and wing size upon ω_{max} and Γ_a, we computed normalized (Spedding et al., 2003a; Hedenström et al., 2006), dimensionless values $\omega_{max}cU_b^{-1}$ and $\Gamma_a(cU_b)^{-1}$, where c is average chord length (Table 1; m) and U_b is body velocity (m s^{-1}) as measured from 3D kinematics (Segre, 2006) (Table 2).

Statistical analysis

We used one-way analysis of variance (ANOVA, d.f.=2,6) to test for an effect of age class upon observed differences in mean ω_{max}, Γ_a, α_s and U_{ind}, U_v and S during WAIR. We used a paired t-test (d.f.=1) to test for significant differences between these same variables measured in adults during WAIR and flight. Values are reported as means ± s.d.

Results

The downstroke was the only portion of the wingbeat during which lift was produced by the wings during WAIR and during flight (Figs 3–6). Our parasagittal, mid-wing samples of the wake revealed cross-sections of what we interpreted to represent starting and ending vortex cores (Γ_a^- and Γ_a^+; Fig. 3). Beginning at 7 d.p.h. (Fig. 4A,B), babies consistently exhibited wake structures similar to those of juveniles and adults (Fig. 4C–F). In contrast, at 6 d.p.h. (Fig. 6), the babies

Table 3. *Data from the wake of Alectoris chukar engaged in wing-assisted incline running (WAIR) and flight*

	Age class				
Variable	Baby	Juvenile	Adult	Adult (flight)	P-value
Vorticity, peak negative (ω_{max}^-; s^{-1})	–595±45	–575±117	–991±507	–737±1	0.1615
Vorticity, peak positive (ω_{max}^+; s^{-1})	510±77	466±75	813±502	817±67	0.2325
Circulation, negative (Γ_a^-; m^2 s^{-1})	–0.18±0.06	–0.98±0.08	–1.8±0.3	–2±1	0.0002
Circulation, positive (Γ_a^+; m^2 s^{-1})	0.20±0.04	1.1±0.2	1.6±0.1	2.8±0.8	0.0002
Impulse angle to horizontal (α_h; deg.)	42±6	41±6	51±2	85+1	0.2076
Impulse angle to substrate (α_s; deg.)	23±6	31±9	29±2	85±1	0.5296
Induced velocity (U_{ind}; m s^{-1})	2.1±0	5.6±0.5	8±2	8.1±0.1	0.0052
Wake vortex velocity (U_v; m s^{-1})	0.23±0.03	1.0±0.2	1.2±0.5	1.2±0.3	0.0165
Wake vortex width (S; m)	0.038±0.005	0.12±0.02	0.15±0.05	0.143±0.006	0.0067

Values are mean ± s.d., N=2 babies, 5 juveniles and 2 adults, except for wake vortex velocity where N=2 juveniles. P values from ANOVA for WAIR data only (d.f. 2, 6).

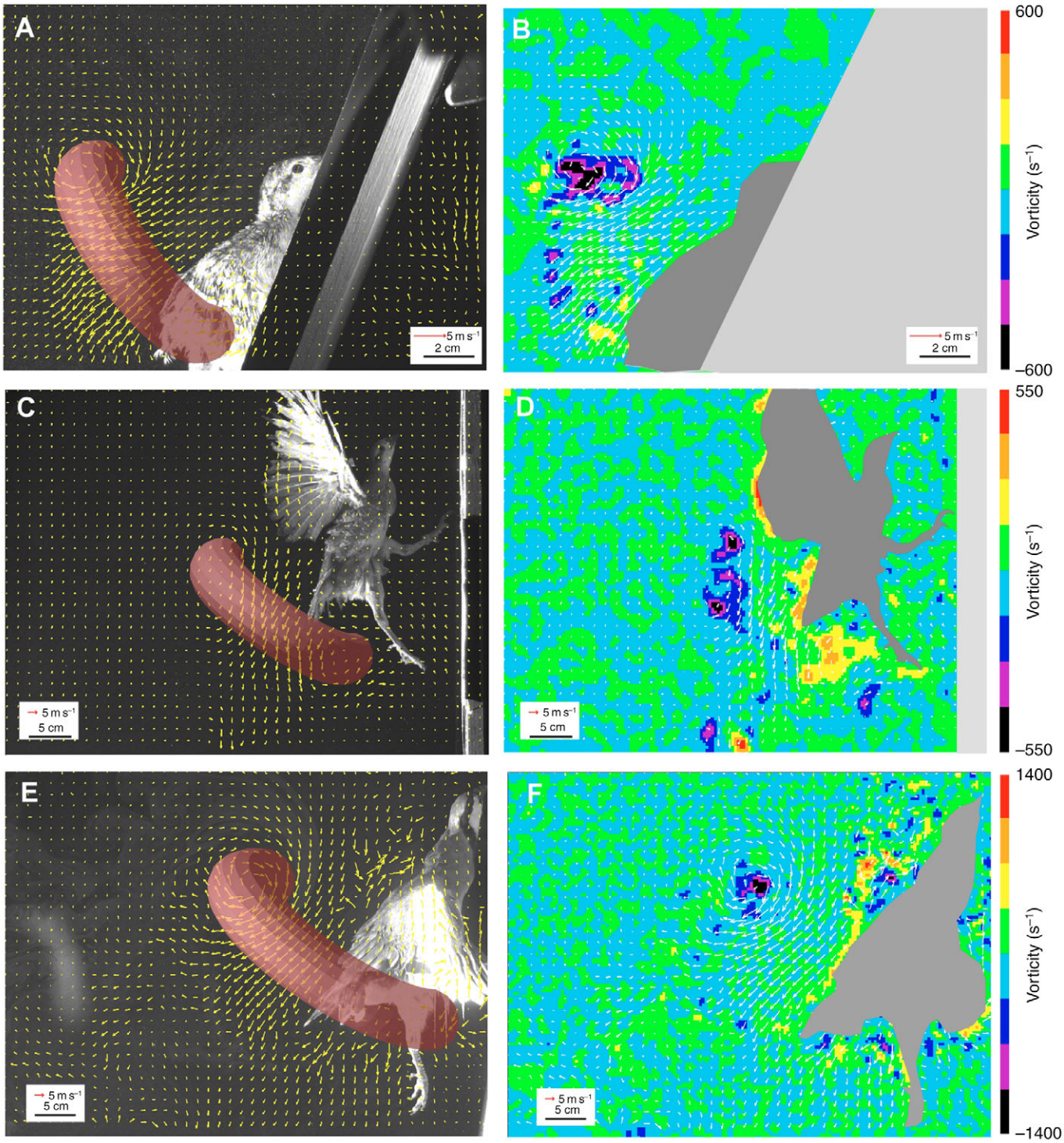

Fig. 4. Velocity fields in the wake of chukar *Alectoris chukar* during WAIR as revealed using DPIV. Backgrounds in (A,C,E) illustrate the bird and incline and in (B,D,F) represent vorticity (ω). Transparent red loops represent an assumed 3D shape of vortex rings as inferred from concentrations of ω about ω^{-}_{max} and ω^{+}_{max} in the DPIV images. (A,B) Baby, ascending at 65°. (C,D) Juvenile ascending at 90°. (E,F) Adult, ascending at 80°. Both starting and ending vortex cores, evident as concentrations of ω^{-} and ω^{+}, respectively, are visible for the wake of the juvenile, whereas the wings and body mask ending vortices in baby and adult. Erroneous vectors due to the DPIV algorithm are apparent above the back of the adult in E.

obviously struggled to climb the slope (65°) and exhibited a wake with less Γ^{-}_{a} (40.5%). During WAIR, impulse from the downstroke was directed upward relative to the ground (average α_h, 45±6°) and also toward the surface of the slope that the animal was climbing, with α_s varying from 23±6° to 31±9°. Average α_s was slightly lower in babies compared to

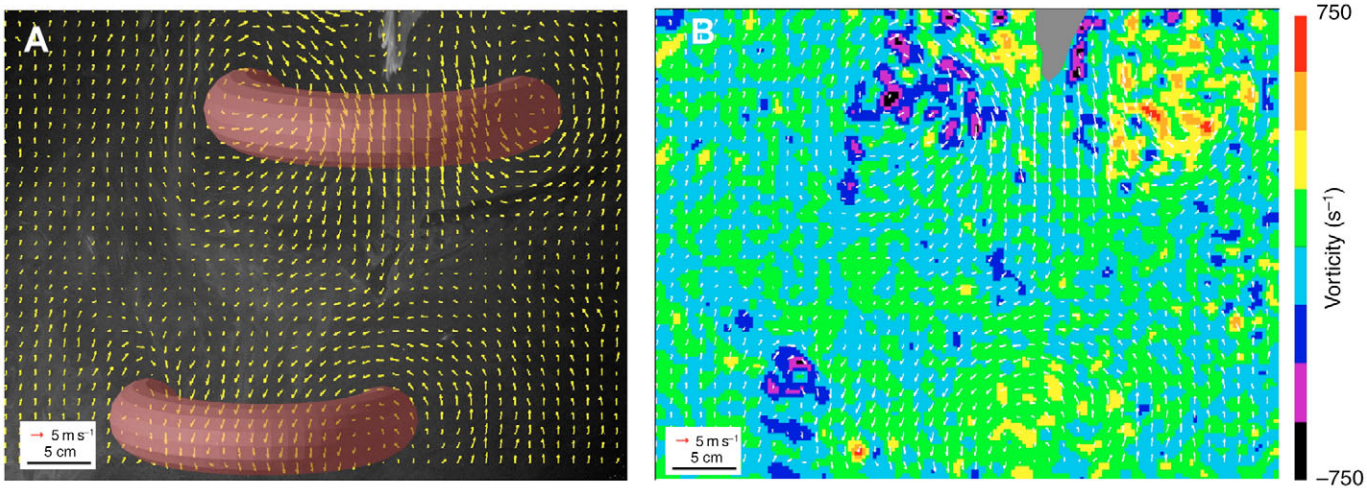

Fig. 5. Velocity fields in the wake of an adult chukar *Alectoris chukar* during ascending flight at 80°, revealed using DPIV. Backgrounds illustrate the bird (A) and vorticity, ω (B). Transparent red loops in A represent an assumed 3D shape of vortex ring as inferred from concentrations of ω about ω^{-}_{max} and ω^{+}_{max}. Effects of two downstrokes are shown, with starting and ending vortex cores evident as concentrations of ω^{-} and ω^{+}, respectively, in B.

juveniles and adults, but the observed differences were not significant (Table 3). During flight, impulse was nearly normal to the ground (85.0±0.5°; Fig. 4). Considering the ground to represent substrate during flight, there was a significant difference between mean α_s during WAIR and flight (P=0.0235). Consistent with large differences in body mass and wing size, Γ^{-}_{a} and Γ^{+}_{a} varied significantly among age classes (P=0.0002; Table 3). Comparing babies and adults engaged in WAIR, Γ^{+}_{a} varied from –0.18±0.06 $m^2\ s^{-1}$ to –1.8±0.3 $m^2\ s^{-1}$, and Γ^{+}_{a} varied from 0.20±0.04 $m^2\ s^{-1}$ to 1.6±0.1 $m^2\ s^{-1}$. Normalizing Γ to remove the effects of c and U_b, removed the significant effect of age class during WAIR (Fig. 7A). Among all three age classes, normalized Γ^{-}_{a} was 14±3 and Γ^{+}_{a} was 14±4. An average of 54±28% more Γ was present in the vortex cores during flight compared with WAIR in adults (Table 3; Fig. 7A), but the differences between means were not statistically significant (P=0.3431 for Γ^{-}_{a} and P=0.3130 for Γ^{+}_{a}).

Age class did not have a significant effect upon absolute or normalized ω^{-}_{max} and ω^{+}_{max} (Table 3). Average ω^{-}_{max} was –724±192 s^{-1}, and average ω^{+}_{max} was 652±189 s^{-1}. Normalized mean ω^{-}_{max} and ω^{+}_{max} were 41±18 and 37±17, respectively.

Induced velocity in the center of the vortex loops varied significantly among age classes (P=0.0052) with a minimum of 2.1±0 m s^{-1} in babies to 8±2 m s^{-1} in adults. Compared with U_{ind} during WAIR, U_{ind} during flight was slightly higher

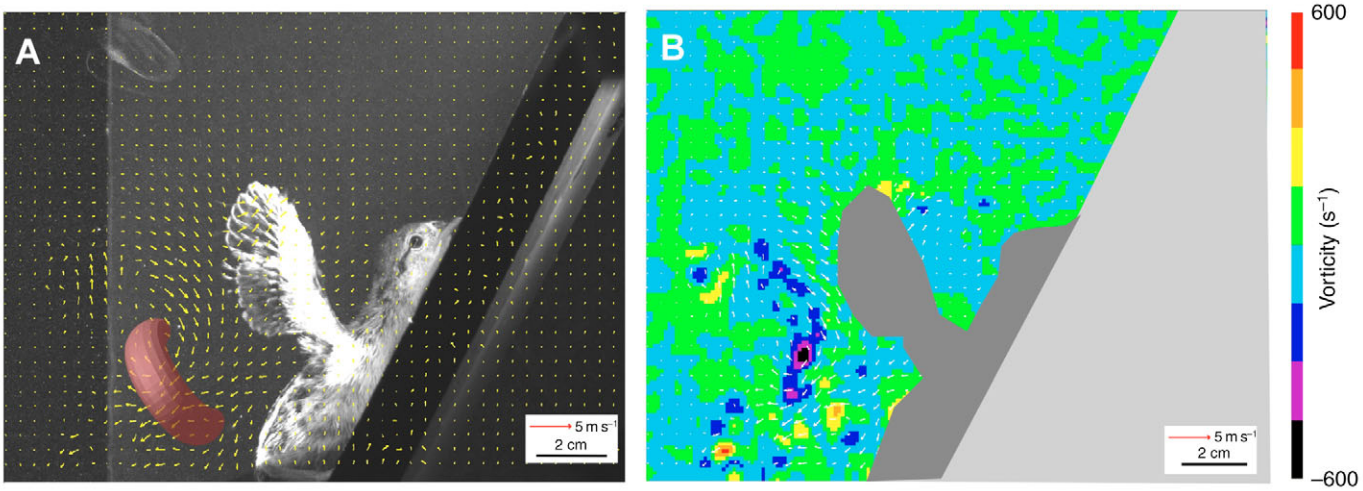

Fig. 6. Velocity fields, revealed using DPIV, of the wake of a baby chukar *Alectoris chukar*, 6 d.p.h., which was obviously struggling during WAIR at 65°. Backgrounds illustrate the bird (A) and vorticity, ω (B). Transparent red loop in A is an assumed 3D shape of vortex ring as inferred from concentrations of ω about ω^{-}_{max} and ω^{+}_{max}. Only a starting vortex (ω^{-}_{max}) is visible. Compared with the wake of the baby in Fig. 3A,B (day 7, post-hatching), the wake is less organized and negative circulation (Γ^{-}_{a}) is less (40.5%).

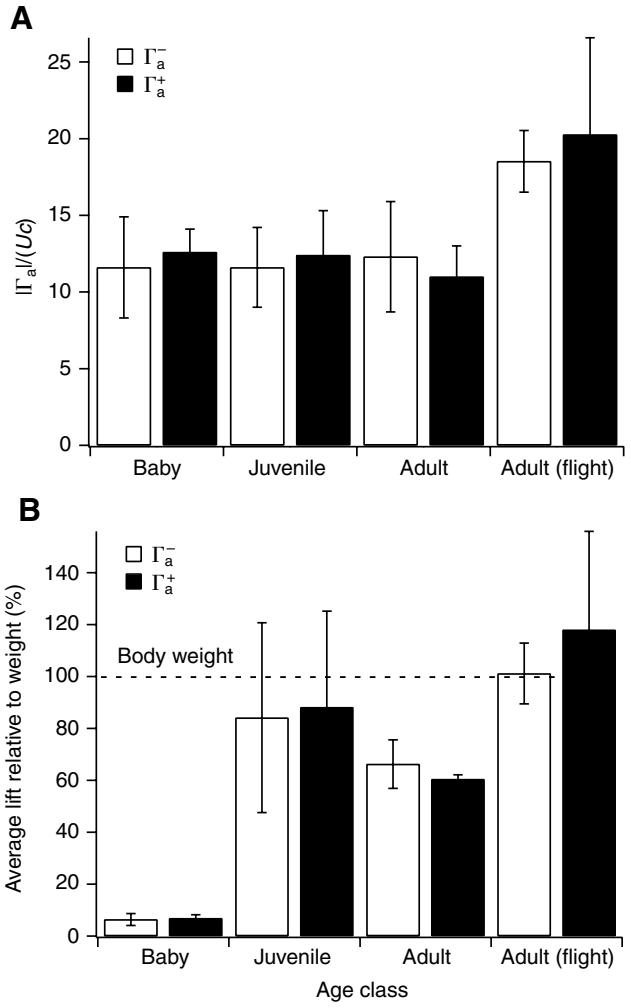

Fig. 7. Normalized circulation (A) and an estimate of average lift relative to weight (B) in different age classes of chukar *Alectoris chukar* engaged in WAIR and in adults during ascending flight. Values are means ± s.d. (*N*=2 babies, 5 juveniles, 2 adults).

(8.1±0.1 m s^{-1}), but the difference between means was not significant (*P*=0.8233). Significant differences were also observed among age classes for wake vortex velocity (U_v, *P*=0.165) and width (*S*, *P*=0.0067).

Wake vortex ratio, W_a, varied from 0.03±0.01 in babies to 0.08±0.02 in both juveniles and adults during WAIR. The observed differences among the age classes were significant when either Γ_a^- (*P*=0.0285) or Γ_a^+ (*P*=0.0156) were employed as the denominator of Eqn 2. W_a averaged 0.05±0.00 during chukar flight.

Expressed relative to body weight, estimated average lift was least in babies during WAIR (Fig. 6B) at 6±2% of body weight when *L* was calculated using Γ_a^- and 7±1% when *L* was calculated using Γ_a^+ in Eqn 1. Relative *L* was slightly greater in juveniles compared with adults (Fig. 6B). For example, based on Γ_a^+, relative *L* in adults was 60±2% and 88±37% in juveniles. The percentage of body weight supported during flight was estimated as 101±12% employing Γ_a^- and 118±37% when using Γ_a^+. Given the downstroke fractions within the entire wingbeat (Segre, 2006) (Table 2), average lift during downstroke L_d=2.3*L* among the three age classes when engaged in WAIR, and L_d=2.2*L* during flight in adults.

Discussion

Our DPIV data provide new evidence that chukar use their wings to produce lift during WAIR, and that the impulse from downstroke is oriented so as to accelerate the body of the animal both upward and toward the substrate it is climbing (Table 1; Figs 4, 6 and 7). Coupled with data from kinematic studies (Dial, 2003; Dial et al., 2006; Segre, 2006), our results revealed a wake dominated by the effects of lift production as in flapping flight in birds (Spedding et al., 2003a; Spedding et al., 2003b; Warrick et al., 2005) (Figs 3–6) rather than a drag-based wake such as might be produced by a paddling motion (Johannson and Lauder, 2004). This is because observed impulse angles (α_h and α_s, Figs 2–6) were nearly perpendicular to the path of wing motion. Specifically, Segre measured stroke plane angles during WAIR at 61° relative to horizontal (Segre, 2006), and our measure of vortex inclination angle (β; orthogonal to α_h and α_s, Fig. 2) was 45±6°. If the wake was being generated solely by drag, we would have observed shear layers in the flow manifest as a street of opposite-sign ω parallel with β (Johannson and Lauder, 2004; Spedding et al., 2003b). Undoubtedly, the wings were producing lift and experiencing profile drag simultaneously (Shultz and Webb, 2002), but the overwhelming pattern of lift-induced wake vortices obscured any measurable traces of profile drag in the wake.

Although our data from direct visualization of the wake are in general agreement with the conclusions of previous experiments that include kinematic and accelerometer measurements (Bundle and Dial, 2003; Dial, 2003; Dial et al., 2006; Segre, 2006), some discrepancies refine our understanding of the mechanics of WAIR and present questions for further study. The DPIV data support the hypothesis that the wings contribute to hindlimb function during WAIR. For adult chukar during WAIR, accelerometer measurements indicated an average force from the wings at 220% of body weight and oriented at 28° relative to the substrate being climbed at an incline of 54° [average taken among four phases of downstroke in table 3 of Bundle and Dial (Bundle and Dial, 2003)]. In comparison, our estimate of L_d in adult WAIR was less at 146±21% of body weight when we used Γ_a^- to estimate L_d and 134±4% when we used Γ_a^+, but the impulse angle (α_s, 29±2°) was within 1 s.d. of that measured by Bundle and Dial (Bundle and Dial, 2003). The accelerometer and DPIV data both serve to revise prior estimates from 2D kinematics (Dial, 2003) that lift is directed perpendicularly toward the substrate.

There are several potential explanations for our lower estimate of L_d compared to the body accelerations measured by Bundle and Dial (Bundle and Dial, 2003). Foremost, the contribution of wing inertia was not subtracted from total

acceleration in the earlier publication (Bundle and Dial, 2003), so their measures include the effects of both aerodynamic forces and wing inertia acting upon the body. Future modeling of wing inertia using detailed 3D kinematics (Hedrick et al., 2004; Segre, 2006) should test whether the average force acting on the body due to wing inertia is approximately 80% of body weight, as suggested by the difference between accelerations in the earlier publication (Bundle and Dial, 2003) and our estimate of L_d.

Another important consideration is that our estimates of L and L_d were developed with only limited insight into the true 3D geometry of the wake. As described in Materials and methods, the most appropriate method for measuring the spatial distribution of wake vortices requires sampling a time-series of DPIV samples for a Lagrangian analysis in which flow trajectories are measured (Dabiri, 2005; Dabiri et al., 2006; Shadden et al., 2006), ideally in 3D or, more realistically given current DPIV technology, using multiple 2D transects of the wake (Spedding et al., 2003a; Warrick et al., 2005). Our DPIV system samples at a maximum of 5 Hz, so a time-series analysis of individual vortices was not feasible. Additionally, WAIR in chukars is an explosive, short-duration activity with finite repeatability before the birds tire and refuse to cooperate, so it is far from amenable to use the same transect-sampling methods used for DPIV measurements of the wake of highly trained passerines (Passeriformes) flying toward a light source in a wind tunnel (Spedding et al., 2003a; Hedenström et al., 2006) or hummingbirds (Trochilidae) hovering at an artificial feeder (Warrick et al., 2005).

There may also have been a deficit in Γ in the wake relative to the bound Γ on the wings due to rapid decay of Γ in the wake resulting from turbulence (Tytell and Ellington, 2003). Based upon measurements of the onset of turbulence and the corresponding decay of Γ in experimentally induced, laminar vortex rings, Tytell and Ellington (Tytell and Ellington, 2003) suggest that a vortex-ring Reynolds number (*Re*; equal to Γ/ν, where ν is kinematic viscosity, Pa s^{-1}) of approximately 5000 is a practical limit below which wake measurements may accurately represent initial impulse and Γ of a shed vortex ring. A ring *Re* of 5000 would be typical of hovering hawkmoths (*Manduca spp.*) or hummingbirds. For comparison, ring *Re* during WAIR varied from approximately 10 000 in baby chukar to 100 000 in adults, and it was approximately 150 000 during flight in adults.

An argument of an effect of rapid wake decay appears to be undermined by recent observations, including our data from chukars (Figs 5 and 7), that sufficient circulation is present in the wake of flying birds to account for weight support (Spedding et al., 2003b; Warrick et al., 2005; Hedenström et al., 2006). However, during WAIR, it is likely that the proximity of the substrate affected wake dynamics (Doligalski et al., 1994; Han and Cho, 2005) and may have increased vortex instability in ways that are not straightforward to estimate given that the ramps we used for WAIR experiments were relatively narrow and parts of the wings always extended over the edge of the substrate.

Regardless of the potential limitations of our estimate of L, our observations of similar wake structure (Fig. 4) and normalized Γ (Fig. 7A) for WAIR among age classes provides novel insight into the aerodynamics of the developing avian wing. DPIV evidence from four species of passerines in flight (Hedenström et al., 2006) similarly indicates that normalized circulation is not sensitive to wing shape (Hedenstrom et al., 2006). Even though baby chukars cannot fly at 6–8 d.p.h. (Dial et al., 2006; Segre, 2006), they were able to generate Γ using their wings as an airfoil in the same way as juveniles and adults. Variation in the magnitude of Γ was associated with learning to effectively perform WAIR during the critical transition stage that occurred at days 6 and 7 post-hatching (Fig. 6). Although absolute Γ increased with increasing size among the three age classes (Table 3; Fig. 7A), normalizing Γ and, thereby, controlling for the effects of c and U_b, revealed that the dramatic differences in feather morphology between baby and adult chukar (Fig. 1) did not have a significant effect upon Γ (Fig. 7A). It is imperative to note that large variance within age classes meant that the power was extremely low ($\leqslant$0.08) for this test of statistical significance. Thus, a larger sample size is needed to confirm that no true difference exists among age classes.

Instead of a deficit of Γ, the comparatively poor performance of baby chukar with respect to L (Fig. 7B) may be attributed to their wing kinematics that we used to calculate A and T in Eqn 1 (Segre, 2006) (Table 2). During WAIR, baby chukar have wingbeats of lower frequency and amplitude than juveniles and adults (Segre, 2006), which led to relatively small A and large T (Table 1). In contrast, the expected trend derived from interspecific scaling of wingbeat kinematics with body size in galliform birds would suggest that babies should have a relatively higher frequency and approximately the same amplitude of wingbeat as the larger birds (Tobalske and Dial, 2000). Ultimately neuromuscular control and the ability to generate work and power using the primary downstroke muscle, the pectoralis, drives the motion of the wing (Dial, 1992; Tobalske et al., 2003; Hedrick et al., 2003). Thus, the observed similarity in normalized Γ among age classes (Fig. 7A) leads us to predict that the performance of the developing wing during WAIR is constrained primarily by control or the ability to generate power rather than shape of the animal's aerofoil.

Understanding the function of morphing structures during transitional stages is critical to evaluating adaptation in ecological and evolutionary time (Bock, 1965; Dial, 2003; Dial et al., 2006). Our data show that a developing wing with symmetrical, partially emerged feathers can develop Γ similar to a wing with asymmetric feathers on an adult wing (Figs 1 and 4). Although understanding the neuromuscular control and power output of the muscles moving these wings awaits further study, the aerodynamics that we report should aid in providing a new model for developing hypotheses about the role of feathers and flight ability of the ancestors of modern birds (Padian and Chiappe, 1998; Prum, 1999; Padian, 2001; Zhou, 2004).

List of symbols and abbreviations

c	average chord length
$\bar{c}$	added mass coefficient
DPIV	digital particle image velocimetry
d.p.h.	days post hatching
L	average lift during wingbeat
L_d	average lift during downstroke
A	loop area of wake vortex
S	width of wake vortex
t	time
T	wingbeat duration
T_d	downstroke duration
U_b	body velocity
U_{ind}	induced velocity in the middle of the vortex wake
U_v	wake vortex velocity
ν	kinematic viscosity
W_a	wake vortex ratio
WAIR	wing-assisted incline running
α_h	angle of vortex impulse relative to horizontal
α_s	angle of vortex impulse relative to slope
β	inclination angle of vortex
Γ	circulation
Γ_a	same-sign circulation within 1.5 chord lengths of a vortex core
Γ_c	contiguous same-sign circulation about a vortex core
ρ	air density
ω	vorticity
ω_{max}	peak vorticity

We sincerely thank P. Segre, B. Jackson, J. Hearn, T. Dial and D. Warrick for their assistance during experiments. P. Segre also provided 3D kinematic data for which we are grateful. Supported by NSF grants IOB-0615648 to B.W.T. and IBN-0417176 to K.P.D.

References

Batchelor, G. K. (1967). *An Introduction to Fluid Dynamics*. Cambridge: Cambridge University Press.

Bock, W. J. (1965). The role of adaptive mechanisms in the origin of the higher levels of organization. *Syst. Zool.* **14**, 272-287.

Bundle, M. W. and Dial, K. P. (2003). Mechanics of wing-assisted incline running (WAIR). *J. Exp. Biol.* **206**, 4553-4564.

Dabiri, J. O. (2005). On the estimation of swimming and flying forces from wake measurements. *J. Exp. Biol.* **208**, 3519-3532.

Dabiri, J. O., Colin, S. P. and Costello, J. H. (2006). Fast-swimming hydromedusae exploit velar kinematics to form an optimal vortex wake. *J. Exp. Biol.* **209**, 2025-2033.

Dial, K. P. (1992). Activity patterns of the wing muscles of the pigeon (*Columba livia*) during different modes of flight. *J. Exp. Zool.* **262**, 357-373.

Dial, K. P. (2003). Wing-assisted incline running and the evolution of flight. *Science* **299**, 402-404.

Dial, K. P., Randall, R. J. and Dial, T. R. (2006). What use is half a wing in the ecology and evolution of birds? *BioScience* **56**, 437-455.

Doligalski, T. L., Smith, C. R. and Walker, J. D. A. (1994). Vortex interactions with walls. *Annu. Rev. Fluid Mech.* **26**, 573-616.

Ellington, C. P. (1984). The aerodynamics of hovering insect flight. V. A vortex theory. *Philos. Trans. R. Soc. Lond. B Biol. Sci.* **305**, 115-144.

Gould, S. J. and Vrba, E. S. (1982). Exaptation; a missing term in the science of form. *Paleobiology* **8**, 4-15.

Han, C. and Cho, J. (2005). Unsteady trailing vortex evolution behind a wing in ground effect. *J. Aircr.* **42**, 218-227.

Hedenström, A., Griethuijsen, L. V., Rosén, M. and Spedding, G. R. (2006). Vortex wakes of birds: recent developments using digital particle image velocimetry in a wind tunnel. *Anim. Biol.* **56**, 535-549.

Hedrick, T. L., Tobalske, B. W. and Biewener, A. A. (2003). How cockatiels (*Nymphicus hollandicus*) modulate pectoralis power output across flight speeds. *J. Exp. Biol.* **206**, 1363-1378.

Hedrick, T. L., Usherwood, J. R. and Biewener, A. A. (2004). Wing inertia and whole-body acceleration: an analysis of instantaneous aerodynamic force production in cockatiels (*Nymphicus hollandicus*) flying across a range of speeds. *J. Exp. Biol.* **207**, 1689-1702.

Johansson, L. C. and Lauder, G. V. (2004). Hydrodynamics of surface swimming in leopard frogs (*Rana pipiens*). *J. Exp. Biol.* **207**, 3945-3958.

Norberg, U. M. (1990). *Vertebrate Flight: Mechanics, Physiology, Morphology, Ecology and Evolution*. New York: Springer.

Padian, K. (2001). Stages in the origin of bird flight: beyond the arboreal–cursorial dichotomy. In *New Perspectives on the Origin and Early Evolution of Birds* (ed. J. A. Gauthier), pp. 255-272. New Haven: Yale University Press.

Padian, K. and Chiappe, L. M. (1998). The origin of birds and their flight. *Sci. Am.* **278**, 38-47.

Prum, R. O. (1999). The development and evolutionary origin of feathers. *J. Exp. Zool.* **285**, 291-306.

Raffel, M., Willert, C. and Kompenhans, J. (2000). *Particle Image Velocimetry: A Practical Guide*. Berlin: Springer-Verlag.

Rayner, J. M. V. (1988). Form and function in avian flight. *Curr. Ornithol.* **5**, 1-66.

Sane, S. P. (2006). Induced airflow in flying insects I. A theoretical model of the induced flow. *J. Exp. Biol.* **209**, 32-42.

Schultz, W. W. and Webb, P. W. (2002). Power requirements of swimming: do new methods resolve old questions? *Integr. Comp. Biol.* **42**, 1018-1025.

Segre, P. S. (2006). A 3-dimensional evaluation of wing movement in ground birds during flap-running and level flight: an ontogenetic study. MS thesis, University of Montana, USA.

Shadden, S. C., Dabiri, J. O. and Marsden, J. E. (2006). Lagrangian analysis of fluid transport in empirical vortex ring flows. *Phys. Fluids* **18**, 047105.

Spedding, G. R., Rosén, M. and Hedenström, A. (2003a). A family of vortex wakes generated by a thrush nightingale in free flight in a wind tunnel over its entire natural range of flight speeds. *J. Exp. Biol.* **206**, 2313-2344.

Spedding, G. R., Hedenström, A. and Rosen, M. (2003b). Quantitative studies of the wakes of freely flying birds in a low-turbulence wind tunnel. *Exp. Fluids* **34**, 291-303.

Tobalske, B. W. and Dial, K. P. (2000). Effects of body size on take-off flight performance in the Phasianidae (Aves). *J. Exp. Biol.* **203**, 3319-3332.

Tobalske, B. W., Hedrick, T. L., Dial, K. P. and Biewener, A. A. (2003). Comparative power curves in bird flight. *Nature* **421**, 363-366.

Tytell, E. D. and Ellington, C. E. (2003). How to perform measurements in a hovering animal's wake: physical modelling of the vortex wake of the hawkmoth, *Manduca sexta*. *Philos. Trans. R. Soc. Lond. B Biol. Sci.* **358**, 1559-1566.

Warrick, D. R., Tobalske, B. W. and Powers, D. R. (2005). Aerodynamics of the hovering hummingbird. *Nature* **435**, 1094-1097.

Zhou, Z. (2004). The origin and early evolution of birds: discoveries, disputes, and perspectives from fossil evidence. *Naturwissenschaften* **91**, 455-471.